JHEP

Published by Institute of Physics Publishing for SISSA

Received: *July 25, 2006*
Revised: *November 6, 2006*
Accepted: *December 22, 2006*
Published: *January 9, 2007*

Quasinormal frequencies and thermodynamic instabilities for the stationary axisymmetric Einstein-Maxwell dilaton-axion black hole

Qiyuan Pan and Jiliang Jing*

Institute of Physics and Department of Physics, Hunan Normal University, Changsha, Hunan 410081, P.R. China
E-mail: panqiyuan@126.com, jljing@hunnu.edu.cn

Abstract: The massless scalar quasinormal frequencies of a stationary axisymmetric Einstein-Maxwell dilaton-axion (EMDA) black hole are investigated by using Leaver's continued fraction method. It is shown that in the complex plane the frequencies move counterclockwise and get a spiral-like shape as the angular momentum per unit mass a increases to its extremal value or the dilaton D decreases to its extremal value for the rotating black hole. However, for the non-rotating Garfinkle-Horowitz-Strominger dilaton (GHSD) black hole, the dilaton parameter D, which is related to the electric charge of this EMDA black hole, cannot make the frequencies spire in the complex ω plane, which is qualitatively different from the charge of the Reissner-Nordström (RN) black hole. The so-call "Spiral-like Criterion" is obtained and it points out that the frequencies won't spire in the complex ω plane if the heat capacity for the considered black hole is always negative and vice versa. The most interesting outcome of our calculation is that the critical point, at which the imaginary part of the wave function related to time-dependent part ($e^{-i\omega t}$) begins to oscillate obviously for the given quantum number, is just the second order phase transition point of Davies. The fact seems to imply that there is some relation between the dynamical evolution and thermodynamic instabilities for the black hole.

Keywords: Black Holes, Black Holes in String Theory, Classical Theories of Gravity.

*Corresponding author

JHEP01(2007)044

Contents

1. Introduction

It is well known that the quasinormal frequencies have become astrophysically significant with the realistic possibility of gravitational wave detection because they provide us the information about the main parameters of a black hole such as its mass M, charge Q and angular momentum per unit mass $a \equiv J/M$ [1, 2]. In addition, the study of the quasinormal frequencies for the highly damped modes may lead to a deeper understanding of the thermodynamic properties of black holes in loop quantum gravity since the real part of quasinormal frequencies with a large imaginary part for the scalar field in the Schwarzschild black hole is equal to the Barbero-Immirzi parameter which is introduced by hand in order that the loop quantum gravity reproduces correct entropy of the black hole [3, 4], and the quasinormal frequencies of anti-de Sitter black holes have a direct interpretation in terms of the dual conformal field theory [5 – 7]. Thus, quasinormal frequencies for various black holes have been studied extensively [8]–[26].

After Regge and Wheeler first studied the linear perturbations of static black holes in 1957 [8], people proposed different methods to obtain the quasinormal frequencies [9 – 11, 1]. In 1985, Leaver presented a continued fraction method for calculating the quasinormal frequencies of both static and rotating black holes [12]. Then, Onozawa et al improved this method for the extreme case in 1996 [13]. Leaver's method provides extremely accurate values for the quasinormal frequencies of each black hole which involves scalar, electromagnetic and gravitational perturbations [14, 15]. Recently it has been extended to compute the Dirac quasinormal frequencies [16 – 19]. Although there are several methods to precisely get the quasinormal frequencies of static black holes, the continued fraction method

is the only one which can be generalized to the rotating cases, such as the Kerr [14] and Kerr-Newman (KN) black holes [15, 18], where besides the quasinormal frequencies we must evaluate the separation constants which are the angular eigenvalues associated with the Teukolsky equations. And as far as we know nobody use this method to study the rapidly damped modes of a dilaton black hole.

Nowadays, it seems that the superstring theory is the most promising candidate for a consistent quantum theory of gravitation. Thus, many people have begun to investigate the quasinormal frequencies of dilaton black holes [21 – 26]. For instance, Konoplya explored the quasinormal frequencies of the electrically charged dilaton black hole and found the effect of the dilaton parameter on quasinormal frequencies. However, they only discussed the quasinormal frequencies of the static, spherically symmetric black holes. So it is worthwhile to extend the investigation to quasinormal frequencies of the dilaton black hole being the stationary axisymmetric solution of the so-called low-energy string theory [27, 28] and to see how they differ from the KN black hole as a result of different horizons and singularities as compared to the KN black hole [15, 18].

On the other hand, one of important characteristics of a black hole is its thermodynamic property. For the static, spherically symmetric Schwarzschild black hole, the heat capacity of the black hole is always negative and the black hole is thermodynamically unstable. But for the static, spherically symmetric and charged Reissner-Nordström (RN) black hole, rotating Kerr black hole, and more general KN black hole, their heat capacities are positive in some parameter regions and negative in other regions. Davies pointed out that the phase transition appears in black hole thermodynamics and the second order phase transition point is the one where the heat capacity diverges [29 – 31]. As one knows, the quasinormal frequencies of a black hole can test the stability of the spacetime against small perturbation [1]. Thus, when we study the dynamical evolution of the external field perturbation around this EMDA black hole, we also discuss some important thermodynamic properties of this black hole and try to find out whether there is some relation between them.

The organization of this paper is as follows. In section 2 the wave equations of this stationary axisymmetric EMDA black hole with a massless scalar field are obtained. In section 3 a short description of the continued fraction method is given. In section 4 the numerical results for the quasinormal frequencies of this considered black hole are presented. In section 5 some relation between the dynamical evolution and thermodynamic instabilities is shown. We summarize and discuss our conclusions in the last section.

2. Wave equations of the EMDA black hole

In the Boyer-Lindquist coordinates (t, r, θ, ϕ), the stationary solution for the axisymmetric EMDA black hole is given by [27, 28]

$$ds^2 = -\frac{\Sigma - a^2\sin^2\theta}{\Delta}dt^2 - \frac{2a\sin^2\theta}{\Delta}\left[(r^2 - 2Dr + a^2) - \Sigma\right]dtd\varphi + \frac{\Delta}{\Sigma}dr^2 + \Delta d\theta^2 + \frac{\sin^2\theta}{\Delta}\left[(r^2 - 2Dr + a^2)^2 - \Sigma a^2\sin^2\theta\right]d\varphi^2, \tag{2.1}$$

with

$$\Sigma = r^2 - 2Mr + a^2, \quad \Delta = r^2 - 2Dr + a^2\cos^2\theta, \tag{2.2}$$

where the electric charge $Q = \sqrt{2\kappa D(D-M)}$ (with $\kappa = e^{2\Phi_0}$), and D, M and a represent the dilaton, mass and angular momentum per unit mass of the black hole respectively. The Arnowitt-Deser-Misner (ADM) mass is $M_{\rm ADM} = M - D$. If we set $a = 0$, this solution is just the non-rotating Garfinkle-Horowitz-Strominger dilaton (GHSD) metric [27, 32]. Here and hereafter we have taken $G = c = 1$.

Obviously, the stationary axisymmetric EMDA black hole differs considerably from the KN black hole: (1) Two horizons of the KN black hole are given by $r_\pm = M \pm \sqrt{M^2-Q^2-a^2}$, whereas for the EMDA black hole we have $r_\pm = [M_{\rm ADM} - Q^2/(2\kappa M_{\rm ADM})] \pm \sqrt{[M_{\rm ADM} - Q^2/(2\kappa M_{\rm ADM})]^2 - a^2}$; (2) The KN metric has singularities at $r^2 + \cos^2\theta = 0$, but the EMDA black hole has singularities at $r^2 - 2Dr + \cos^2\theta = 0$. Thus, it is worthwhile to investigate the massless scalar quasinormal frequencies of this EMDA black hole in order to see how these differ from the KN black hole.

In the background geometry of this stationary axisymmetric EMDA black hole, a massless scalar field Φ evolves according to the curved space Klein-Gordon equation

$$\frac{1}{\sqrt{-g}}\frac{\partial}{\partial x^\mu}\left(\sqrt{-g}g^{\mu\nu}\frac{\partial\Phi}{\partial x^\nu}\right) = 0, \tag{2.3}$$

where g is the determinant of the metric. We can easily derive the master equation that governs the evolution of massless scalar perturbations of this EMDA spacetime

$$\begin{aligned}&\frac{(r^2-2Dr+a^2)^2 - \Sigma a^2\sin^2\theta}{\Sigma}\frac{\partial^2\Phi}{\partial t^2} - \frac{\partial}{\partial r}\left(\Sigma\frac{\partial\Phi}{\partial r}\right) - \frac{1}{\sin\theta}\frac{\partial}{\partial\theta}\left(\sin\theta\frac{\partial\Phi}{\partial\theta}\right)\\ &-\frac{\Sigma - a^2\sin^2\theta}{\sin^2\theta\Sigma}\frac{\partial^2\Phi}{\partial\varphi^2} + \frac{4a(M-D)r}{\Sigma}\frac{\partial^2\Phi}{\partial t\partial\varphi} = 0.\end{aligned} \tag{2.4}$$

Assuming that the azimuthal and time dependence of our fields will be the form $e^{-i(\omega t - m\varphi)}$, we get the separated differential equation for an angular part of the perturbations

$$[(1-u^2)Y_{lm,u}(u)]_{,u} + (a^2\omega^2u^2 - \frac{m^2}{1-u^2} + A_{\rm lm})Y_{\rm lm}(u) = 0, \tag{2.5}$$

and that for a radial part

$$\left[\frac{d}{dr}\left(\Sigma\frac{d}{dr}\right) + \frac{(r^2-2Dr+a^2)^2\omega^2 - 4a\omega m(M-D)r + a^2m^2}{\Sigma} - A_{\rm lm} - a^2\omega^2\right]R_{\rm lm}(r) = 0, \tag{2.6}$$

where $u = \cos\theta$. Therefore, we will study the quasinormal frequencies of the stationary axisymmetric EMDA black hole with massless scalar fields from eqs. (2.5) and (2.6).

3. The continued fraction method

For this stationary axisymmetric EMDA black hole, in eq. (2.5) $A_{\rm lm}$ is the angular separation constant which can be solved numerically following Leaver [12], and it is reduced to

$l(l+1)$ in the Schwarzschild case. Boundary conditions for eq. (2.5) are that $Y_{\rm lm}(u)$ are finite at the regular singular points $u = \pm 1$, where the indices are given by $\pm m/2$. So a solution to eq. (2.5) can given by

$$Y_{\rm lm}(u) = e^{a\omega u}(1-u^2)^{|m|/2}\sum_{n=0}^{\infty} a_n^\theta (1+u)^n, \tag{3.1}$$

where the superscript θ denotes the association with the angular equation. The expansion coefficients are related by a three-term recurrence relation and the boundary condition at $u = +1$ is satisfied only by its minimal solution sequence. The three-term recurrence relation is expressed as

$$\begin{aligned} &\alpha_0^\theta a_1^\theta + \beta_0^\theta a_0^\theta = 0, \\ &\alpha_n^\theta a_{n+1}^\theta + \beta_n^\theta a_n^\theta + \gamma_n^\theta a_{n-1}^\theta = 0, \qquad (n \geq 1), \end{aligned} \tag{3.2}$$

where

$$\begin{aligned} \alpha_n^\theta &= -2(n+1)(n+|m|+1), \\ \beta_n^\theta &= n(n-1) + 2n(|m|+1-2a\omega) - [2a\omega(|m|+1) - |m|(|m|+1)] - (a^2\omega^2 + A_{\rm lm}), \\ \gamma_n^\theta &= 2a\omega(n+|m|). \end{aligned} \tag{3.3}$$

We will obtain the minimal solution if the angular separation constant $A_{\rm lm}$ is a root of the continued fraction equation

$$0 = \beta_0^\theta - \frac{\alpha_0^\theta\gamma_1^\theta}{\beta_1^\theta -}\frac{\alpha_1^\theta\gamma_2^\theta}{\beta_2^\theta -}\frac{\alpha_2^\theta\gamma_3^\theta}{\beta_3^\theta -}\frac{\alpha_3^\theta\gamma_4^\theta}{\beta_4^\theta -}\cdots . \tag{3.4}$$

It is well known that the quasinormal frequencies are defined to be the modes with purely ingoing waves at the event horizon and purely outgoing waves at infinity [11]. Obviously, the boundary conditions of the wave function $R_{\rm lm}(r)$ at the event horizon ($r = r_+$) and infinity ($r \to +\infty$) for this EMDA black hole can be written as

$$\begin{aligned} R_{\rm lm}(r) &\sim (r-r_+)^{-i\sigma_+}, \qquad r \to r_+, \\ R_{\rm lm}(r) &\sim r^{-1+2i(M-D)\omega} e^{i\omega r}, \qquad r \to \infty, \end{aligned} \tag{3.5}$$

where $\sigma_\pm = \frac{2(M-D)\omega r_\pm - am}{b}$ and $b = 2\sqrt{M^2-a^2}$.

Thus, a solution to eq. (2.6) which satisfies the desired behavior at the boundary should be

$$R_{\rm lm}(r) = e^{i\omega r}(r-r_-)^{-1+2i(M-D)\omega+i\sigma_+}(r-r_+)^{-i\sigma_+}\sum_{n=0}^{\infty} a_n^r \left(\frac{r-r_+}{r-r_-}\right)^n . \tag{3.6}$$

The expansion coefficients here are again defined by a three-term recurrence relation starting with $a_0 = 1$:

$$\begin{aligned} \alpha_0^r a_1^r + \beta_0^r a_0^r &= 0, \\ \alpha_n^r a_{n+1}^r + \beta_n^r a_n^r + \gamma_n^r a_{n-1}^r &= 0, \quad (n \geq 1), \end{aligned} \tag{3.7}$$

where the recurrence coefficients α_n^r, β_n^r and γ_n^r are given in terms of n and the black-hole physical parameters by

$$\begin{aligned}
\alpha_n^r &= n^2 + (c_0 + 1)n + c_0, \\
\beta_n^r &= -2n^2 + (c_1 + 2)n + c_3, \\
\gamma_n^r &= n^2 + (c_2 - 3)n + c_4 - c_2 + 2,
\end{aligned} \tag{3.8}$$

with

$$\begin{aligned}
c_0 &= 1 - 2i(M-D)\omega - \frac{2i}{b}\left[2M(M-D)\omega - am\right], \\
c_1 &= -4 + 2i\omega[4(M-D) + b] + \frac{4i}{b}\left[2M(M-D)\omega - am\right], \\
c_2 &= 3 - 6i(M-D)\omega - \frac{2i}{b}\left[2M(M-D)\omega - am\right], \\
c_3 &= \frac{8(M-D)\omega + 2i}{b}\left[2M(M-D)\omega - am\right] - 1 + i\omega[4(M-D) + b] - 2am\omega \\
&\quad + \omega^2[8(M-D)^2 + 4(M-D)b + 8M(M-D) - a^2] - A_{\mathrm{lm}}, \\
c_4 &= 1 - 8(M-D)^2\omega^2 \\
&\quad - 6i(M-D)\omega - \frac{8(M-D)\omega + 2i}{b}\left[2M(M-D)\omega - am\right].
\end{aligned} \tag{3.9}$$

The radial series solution (3.6) converges and the boundary condition (3.5) is satisfied as the frequency ω is a root of the three-term continued fraction equation

$$0 = \beta_0^r - \frac{\alpha_0^r\gamma_1^r}{\beta_1^r -}\frac{\alpha_1^r\gamma_2^r}{\beta_2^r -}\frac{\alpha_2^r\gamma_3^r}{\beta_3^r -}\frac{\alpha_3^r\gamma_4^r}{\beta_4^r -}\cdots . \tag{3.10}$$

To calculate these quasinormal frequencies using Leaver's continued fraction method, we will seek the roots which satisfy both three-term recurrence relation eqs. (3.4) and (3.10) for a given D, a, l and m.

4. Numerical results

In this section we present the numerical results obtained by using Leaver's continued fraction method. In order to compare with other authors' results, we will take $2M_{\mathrm{ADM}} = 2(M - D) = 1$. Because of $r_\pm = M_{\mathrm{ADM}} + D \pm \sqrt{(M_{\mathrm{ADM}} + D)^2 - a^2}$, we have $(M_{\mathrm{ADM}} + D)^2 > a^2$. Notice that the dilaton parameter D is negative [27, 28] but the angular momentum per unit mass a is positive. Thus, as $D \to 0$ and $a \to 0$ our results reduce to the static Schwarzschild case, as $a \to 0$ reduce to the static GHSD case and $D \to 0$ reduce to the rotating Kerr case. The continued fractions eqs. (3.4) and (3.10) can be evaluated by using an excellent method known as modified Lentz's algorithm [33]. The results will be organized into two subsections: the dependence on the angular momentum per unit mass and the dilaton.

JHEP01(2007)044

a	$D=0$	$D=-0.1$	$D=-0.15$	$D=-0.2$	$D=-0.25$
0	0.220910-0.209791i	0.238212-0.213368i	0.248595-0.215288i	0.260585-0.217266i	0.274736-0.219234i
0.1	0.221535-0.209025i	0.239050-0.212110i	0.249579-0.213604i	0.261746-0.214915i	0.276091-0.215755i
0.15	0.222315-0.208017i	0.240077-0.210417i	0.250757-0.211294i	0.263058-0.211596i	0.277350-0.210610i
0.2	0.223398-0.206506i	0.241452-0.207790i	0.252238-0.207606i	0.264386-0.206060i	0.277067-0.201490i
0.25	0.224762-0.204366i	0.243020-0.203880i	0.253553-0.201874i	0.263845-0.197008i	-
0.3	0.226341-0.201397i	0.244284-0.198055i	0.252769-0.192983i	-	-
0.35	0.227958-0.197264i	0.243279-0.189363i	-	-	-
0.4	0.229074-0.191402i	-	-	-	-
0.45	0.227695-0.183138i	-	-	-	-
0.49	0.221229-0.178964i	-	-	-	-
a	$D=-0.3$	$D=-0.35$	$D=-0.4$	$D=-0.45$	$D=-0.49$
0	0.291943-0.221038i	0.313799-0.222295i	0.343595-0.221904i	0.390392-0.215480i	0.471221-0.180477i
0.1	0.293390-0.215417i	0.314334-0.211793i	-	-	-
0.15	0.293347-0.206453i	-	-	-	-
≥ 0.2	-	-	-	-	-

Table 1: Fundamental scalar quasinormal frequencies of the EMDA metric with $l = m = 0$ for selected values of the dilaton and angular momentum per unit mass. Dashed entries in this table correspond to combinations of D and a for which $(M_{\rm ADM} + D)^2 \leq a^2$.

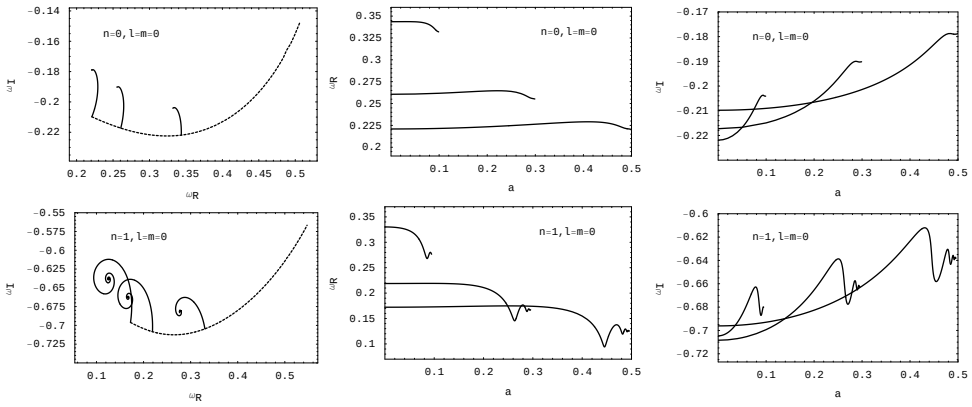

Figure 1: Left two panels show trajectories in the complex ω plane of the first two scalar quasinormal frequencies of the EMDA black hole for $l = m = 0$. In each panel, the bottom dashed line corresponds to modes of non-rotating GHSD black hole, i.e., $a = 0$ and $D = 0 \to -0.5$. The other three lines from left to right on this dashed line correspond to modes of increasing a from zero to its extremal value for $D = 0$, -0.2 and -0.4 respectively. The other panels draw the real part ω_R and imaginary part ω_I of the quasinormal frequencies versus a. These panels tell us that, for $l = m = 0$, both the real and imaginary parts are oscillatory functions of a and the oscillation begins earlier and earlier as the dilaton D decreases from the overtone number $n = 1$.

4.1 Dependence on the angular momentum per unit mass

In table 1 we give numerical results for the fundamental scalar quasinormal frequencies with $l = m = 0$ as a function of the dilaton D and angular momentum per unit mass a. Dashed entries in this table correspond to combinations of D and a for which $(M_{\rm ADM} + D)^2 \leq a^2$.

The scalar quasinormal frequencies of the EMDA black hole for $n = 0,\ 1$ and $l = m = 0$

JHEP01(2007)044

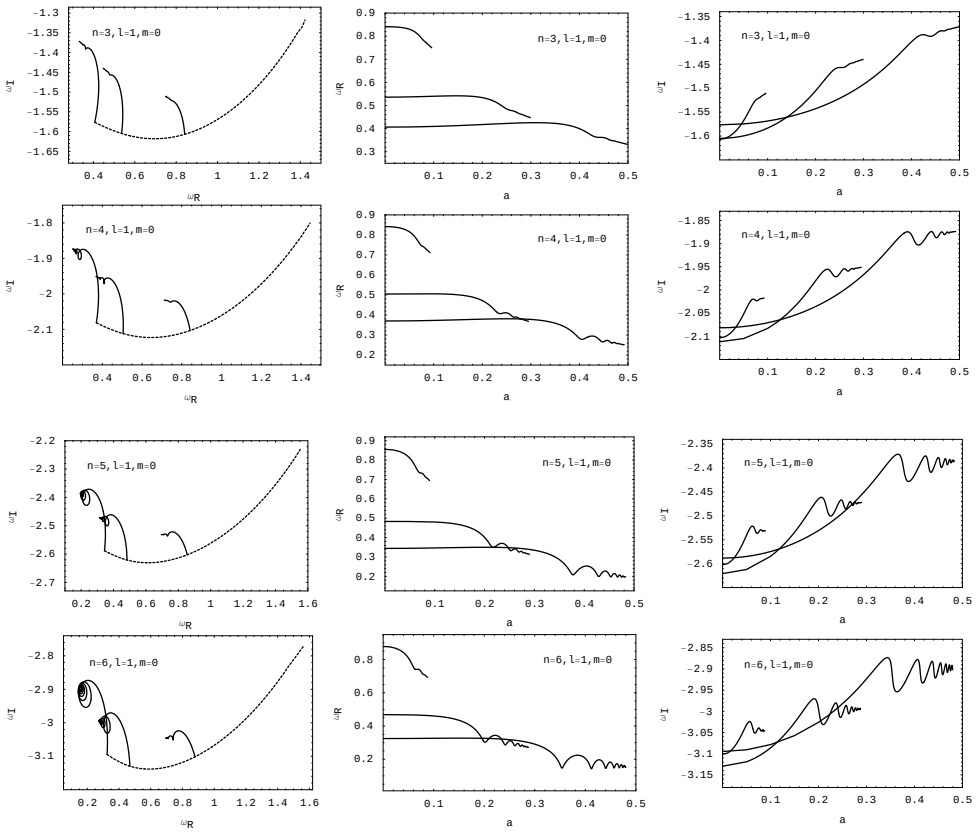

Figure 2: Left four panels describe the behavior of the scalar quasinormal frequencies of the EMDA black hole for $n = 3,\ 4,\ 5$ and 6 in the complex ω plane for $l = 1$, $m = 0$. In each panel, the bottom dashed line corresponds to modes of non-rotating GHSD black hole, i.e., $a = 0$ and $D = 0 \to -0.5$. The other three lines from left to right on this dashed line correspond to modes of increasing a from zero to its extremal value for $D = 0$, -0.2 and -0.4 respectively. The other panels draw the real part ω_R and imaginary part ω_I of the quasinormal frequencies versus a. These panels show that, for $n \geq 4$, both the real and imaginary parts are oscillatory functions of a and the oscillation begins earlier and earlier as the dilaton D decreases or the overtone number n increases with $l = 1$, $m = 0$. For clarity we don't draw modes with other values of m.

are shown by figure 1 and those for $n = 3,\ 4,\ 5,\ 6$ and $l = 1,\ m = 0$ are shown by figure 2. The left columns in the figures 1 and 2 describe the behavior of quasinormal frequencies in the complex ω plane which show that the frequencies generally move counterclockwise as the angular momentum per unit mass a increases (the three lines from left to right on the dashed line). They get a spiral-like shape, moving out of their Schwarzschild ($a = 0$ and $D = 0$) or non-rotating GHSD black hole ($a = 0$ and $D = 0 \to -0.5$) values and "looping in" towards some limiting frequency as the angular momentum per unit mass tends to the extremal value $a - D = 0.5$. For a given angular quantum number l, we observe that the number of spirals increases as the overtone number n increases. Though the dependence of the frequencies on the quantum number l is quite complicated, this conclusion is also true for higher values of l, which agrees with other authors' analysis [14, 15, 18, 19]. However,

JHEP01(2007)044

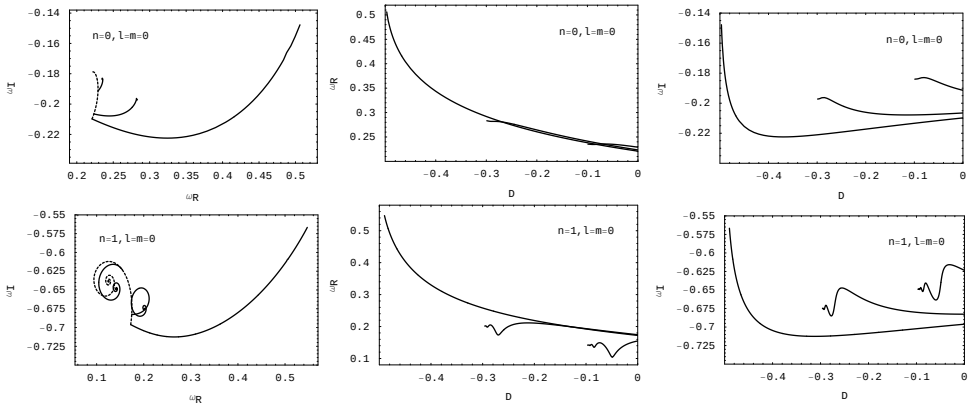

Figure 3: Left two panels show trajectories in the complex ω plane of the first two scalar quasinormal frequencies of the EMDA black hole for $l = m = 0$. In each panel, the left dashed line corresponds to modes of the rotating Kerr black hole, i.e., $D = 0$ and $a = 0 \to 0.5$. The other three lines from bottom to top on this dashed line correspond to modes of decreasing D from zero to its extremal value for $a = 0$, 0.2 and 0.4 respectively. The other panels draw the real part ω_R and imaginary part ω_I of the quasinormal frequencies versus D. These panels tell us that, the dilaton D cannot make the frequencies spire in the complex plane for the non-rotating GHSD black hole, but both the real and imaginary parts are oscillatory functions of D and the oscillation begins earlier and earlier as the angular momentum per unit mass a increases for the rotating black hole (i.e., $a \neq 0$) with $l = m = 0$ from the overtone number $n = 1$.

for a given overtone number n, the increasing l has the effect of "unwinding" the spirals, as we see in the two figures that the spiral begins at $n = 1$ for $l = 0$ but starts at $n = 4$ for $l = 1$ with $m = 0$. The second and last columns in the figures 1 and 2 illustrate that the real and imaginary parts of the quasinormal frequencies are the oscillatory functions of the angular momentum per unit mass a. The oscillation starts earlier and earlier as the overtone number n grows for a fixed l, but it begins later and later as the angular quantum number l increases for a fixed n. Obviously, these properties are similar to the quasinormal frequencies of the KN black hole [15, 18].

4.2 Dependence on the dilaton

Figures 3 and 4 obviously show that the intermediate decay of the massless scalar perturbation around the EMDA black hole depends on the dilaton parameter D. For the non-rotating GHSD black hole ($a = 0$), the real part of the quasinormal frequencies ω_R increases as D decreases, but the imaginary part ω_I decreases first and then increases. Notice that the dilaton parameter D, which is related to the electric charge of this EMDA black hole, cannot make the frequencies spire in the complex ω plane, which is qualitatively different from the charge Q of the RN black hole [19]. However, for the rotating black hole (i.e., $a \neq 0$), it is found that the frequencies generally move counterclockwise as the dilaton D decreases (the two lines from middle to top on the dashed line). They get a spiral-like shape, moving out of their rotating Kerr black hole values and "looping in" towards some limiting frequency as the dilaton tends to the extremal value $a - D = 0.5$. For a given

JHEP01(2007)044

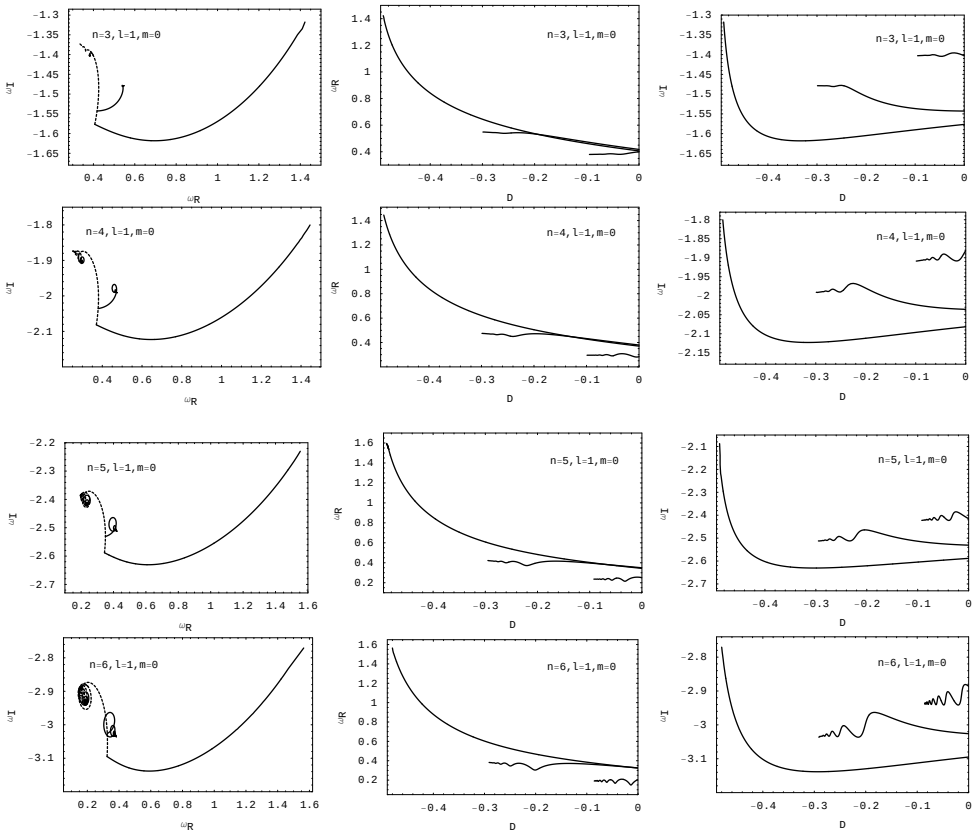

Figure 4: Left four panels describe the behavior of the scalar quasinormal frequencies of the EMDA black hole for $n = 3,\ 4,\ 5$ and 6 in the complex ω plane for $l = 1,\ m = 0$. In each panel, the left dashed line corresponds to modes of the rotating Kerr black hole, i.e., $D = 0$ and $a = 0 \to 0.5$. The other three lines from bottom to top on this dashed line correspond to modes of decreasing D from zero to its extremal value for $a = 0$, 0.2 and 0.4 respectively. The other panels draw the real part ω_R and imaginary part ω_I of the quasinormal frequencies versus D. These panels show that, for $n \geq 4$, the dilaton D cannot make the frequencies spire in the complex plane for the non-rotating GHSD black hole, but both the real and imaginary parts are oscillatory functions of D and the oscillation begins earlier and earlier as the angular momentum per unit mass a increases or the overtone number n grows for the rotating black hole (i.e., $a \neq 0$) with $l = 1,\ m = 0$. For clarity we don't draw modes with other values of m.

angular quantum number l, we observe that the number of spirals increases as the overtone number n increases, which is similar to other authors' work [14, 15, 18, 19]. But for a given overtone number n, the increasing l has the effect of "unwinding" the spirals, as we see in the two figures that the spiral begins at $n = 1$ for $l = 0$ but starts at $n = 4$ for $l = 1$ with $m = 0$. The second and last columns in the figures 3 and 4 illustrate that the real and imaginary parts of the quasinormal frequencies are the oscillatory functions of the dilaton D. The oscillation starts earlier and earlier as the angular momentum per unit mass a increases or the overtone number n grows for a fixed l, but it begins later and later as the angular quantum number l increases for a fixed n. From the previous subsection, it should

JHEP01(2007)044

be noted that the oscillatory functions of the angular momentum per unit mass a depend on the dilaton D, and the oscillation begins earlier and earlier as the dilaton D decreases.

Therefore, our study shows the qualitatively different properties between the dilaton spacetimes in string theory and those appearing in general relativity because of the appearance of dilaton.

5. Spiral-like criterion

From the previous section we know that in the complex plane the frequencies move counterclockwise and get a spiral-like shape as the angular momentum per unit mass a increases to its extremal value or the dilaton D decreases to its extremal value for the rotating black hole, but for the non-rotating Garfinkle-Horowitz-Strominger dilaton (GHSD) black hole, the dilaton parameter D cannot make the frequencies spire in the complex ω plane, which is qualitatively different from the charge of the Reissner-Nordström (RN) black hole [19]. In this section we will give a criterion which can be used to determine whether the frequencies spire or not in the complex ω plane.

It is well known that the heat capacity C_{JQ} of the EMDA black hole is given as [34]

$$C_{JQ} = -T\left(\frac{\partial^2 F}{\partial^2 T}\right)_{J,Q} = \frac{TS^3 M_{\rm ADM}}{\pi J^2 - S^3 T^2}, \tag{5.1}$$

where the Hawking temperature T, angular momentum J, Helmoltz free energy F, and Bekenstein-Hawking entropy of the black hole S are [34]

$$\begin{aligned} T &= \frac{1}{4\pi}\frac{r_+ - r_-}{r_+^2 - 2Dr_+ + a^2}, \quad J = a(M-D) = aM_{\rm ADM}, \\ F &= \frac{1}{2}\left(M_{\rm ADM} - D + \frac{J^2}{M_{\rm ADM}^2 r_+}\right), \quad S = \pi(r_+^2 - 2Dr_+ + a^2). \end{aligned} \tag{5.2}$$

This heat capacity is positive in some parameter region and negative in other region. It is obvious that the divergent point of the heat capacity occurs at $\pi J^2 - S^3 T^2 = 0$. Thus, the top two panels in figure 5 we draw the behavior of the heat capacity C_{JQ} versus a (or D) for some fixed values $D = 0$, -0.2 and -0.4 respectively (or $a = 0$, 0.2 and 0.4 respectively). In each panel, the different vertical lines correspond to the singular points of the heat capacity. It is shown that for the non-rotating GHSD black hole (i.e., $a = 0$), there is no the singular point of the heat capacity and its heat capacity is always negative, which is contrary to other cases. It just corresponds to the conclusion given in the previous section that the dilaton parameter D cannot make the frequencies spire in the complex ω plane for the non-rotating GHSD black hole which is contrary to other cases, i.e., the frequencies move counterclockwise and get a spiral-like shape as the angular momentum per unit mass a increases to its extremal value or the dilaton D decreases to its extremal value for the rotating black hole in figures 1–4. From this fact, we conclude that the frequencies won't spire in the complex ω plane if the heat capacity for the considered black hole is always negative and vice versa. It can be confirmed by other authors' work for

JHEP01(2007)044

Left three panels (D, a)				*Right three panels* (a, D)		
SP	(-0.4 , 0.040)	(-0.2 , 0.178)	(0 , 0.341)	(0 , -)	(0.2 , -0.172)	(0.4 , -)
$CP(l = m = 0, n = 1)$	(-0.4 , 0.040)	(-0.2 , 0.178)	(0 , 0.340)	(0 , -)	(0.2 , -0.183)	(0.4 , -)
$CP(l = 1, m = 0, n = 4)$	(-0.4 , 0.043)	(-0.2 , 0.183)	(0 , 0.341)	(0 , -)	(0.2 , -0.181)	(0.4 , -)

Table 2: The singular point (SP) of the heat capacity and the critical point (CP) at which the imaginary part of the wave function related to time-dependent part for per unit time firstly begins to oscillate for $l = m = 0$ and $l = 1, m = 0$. From the left to right, the value in each bracket corresponds to the different vertical line in figure 5 respectively. Dashed entries in this table correspond to the inexistent points.

Reissner-Nordström (RN) and Kerr-Newman (KN) black hole [14, 15, 18, 19] because the heat capacity is positive in some parameter region [29, 30]

$$C_{JQ} = -T\left(\frac{\partial^2 F}{\partial^2 T}\right)_{J,Q} = \frac{TS^3M}{\pi J^2 + \pi Q^4/4 - S^3T^2}, \tag{5.3}$$

and the frequencies really spire in the complex ω plane when the overtone number n grows to some value for a given quantum number l.

As one knows, the quasinormal frequencies of a black hole can test the stability of the spacetime against small perturbation [1]. Because the wave function related to time-dependent part $\Phi \sim e^{-i\omega t}$ of the massless scalar perturbation depends on ω, we give trajectories of the imaginary part of the wave function related to time-dependent part for per unit time $Im(e^{-i\omega})$ versus a and D for the first oscillation of the scalar quasinormal frequencies of this EMDA black hole with $l = m = 0$ in the middle two panels and $l = 1,\ m = 0$ in the bottom ones of figure 5. In each panel, the different vertical lines correspond to the critical points at which the imaginary part of the wave function related to time-dependent part begins to oscillate obviously.

Considering that we are looking at figure 5, the agreement of the singular point of the heat capacity with the critical point at which the imaginary part of the wave function related to time-dependent part for per unit time begins to oscillate obviously is quite impressive. In order to compare to each other, we present the singular point (SP) of the heat capacity and the critical point (CP) which the imaginary part of the wave function related to time-dependent part begins to oscillate obviously for $l = m = 0$ with $n = 1$ and $l = 1, m = 0$ with $n = 4$ in table 2. It should be noted that the heat capacity is always positive for the cases $a > 0.341$ (for $2M_{\rm ADM} = 1$) with decreasing D from zero to its extremal value, so there is no the singular point (SP) of the heat capacity and the imaginary part of the wave function related to time-dependent part begins to oscillate directly without the critical point (CP) for the case $a = 0.4$ (i.e., the inexistent points (0.4, -)).

From figure 5 and table 2 we find that the singular point of the heat capacity is in good agreement the critical point which the imaginary part of the wave function related to time-dependent part for per unit time begins to oscillate obviously. Because it is difficult to accurately determine the position of these critical points, we can see some of the differences between SP (singular points) and CP (critical points) about 8%. We have checked it and

JHEP01(2007)044

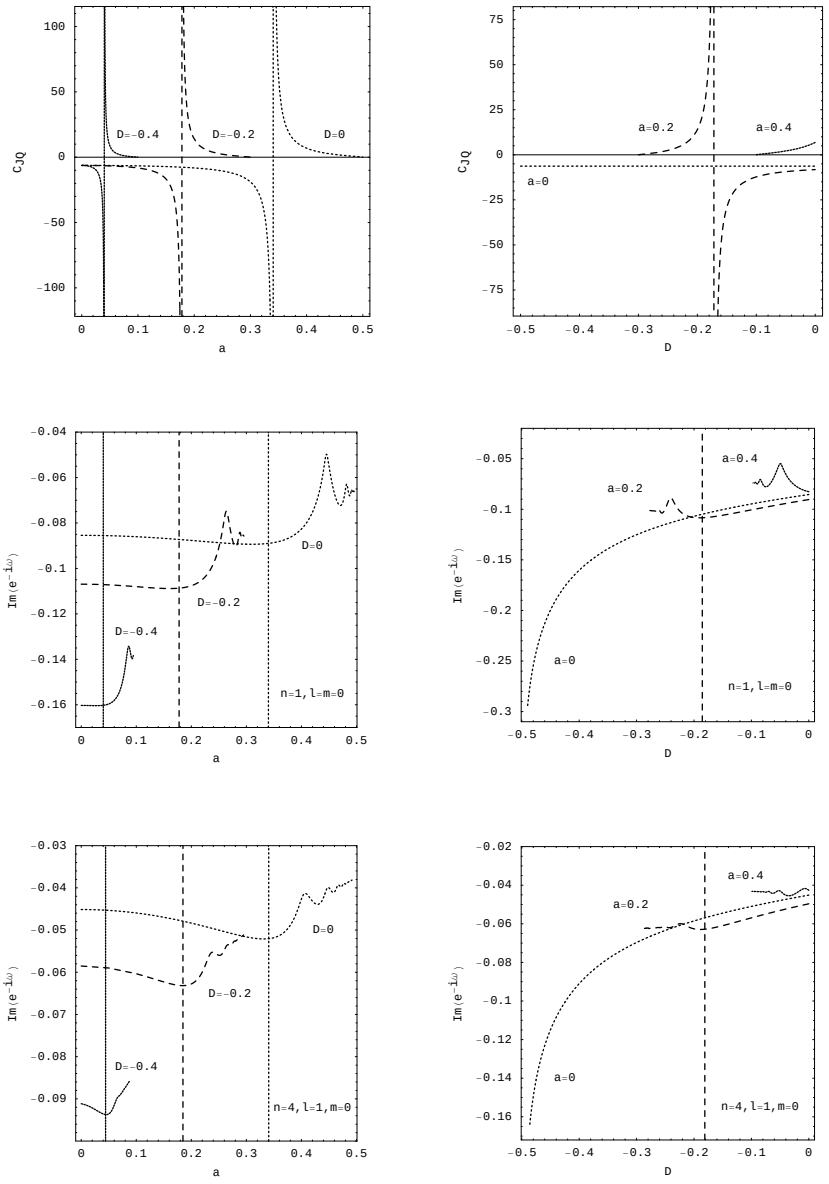

Figure 5: Top two panels describe the behavior of the heat capacity C_{JQ} versus a and D. The other four panels show trajectories of the imaginary part of the wave function related to time-dependent part for per unit time versus a and D for the first oscillation of the scalar quasinormal frequencies of the EMDA black hole with $l = m = 0$ and $l = 1, m = 0$. The different dashed lines correspond to cases of increasing a from zero to its extremal value for $D = 0$, -0.2 and -0.4 respectively in the left three panels, but correspond to cases of decreasing D from zero to its extremal value for $a = 0$, 0.2 and 0.4 respectively in the right ones. The different vertical lines in each panel correspond to the singular points of the heat capacity or the critical points at which the imaginary part of the wave function related to time-dependent part begins to oscillate obviously. These panels tell us that the critical point is just the singular point of the heat capacity, which is the second order phase transition point of Davies.

JHEP01(2007)044

found it available for other cases which the imaginary part of the wave function related to time-dependent part begins to oscillate obviously when the overtone number n grows to some value for a given quantum number l. It is shown that the critical point is just the singular point of the heat capacity, which is the second order phase transition point of Davies [29 – 31]. For the non-rotating GHSD black hole (i.e., the inexistent points (0, -)), there is no the second order phase transition point. The fact seems to imply that there is some relation between the dynamical evolution and thermodynamic instabilities for the black hole which needs to be further investigated.

6. Summary

The massless scalar quasinormal frequencies of the stationary axisymmetric EMDA black hole have been calculated numerically by using Leaver's continued fraction method. The fundamental quasinormal frequencies and the high overtones quasinormal frequencies are obtained. It is shown that in the complex ω plane the frequencies generally move counterclockwise as the angular momentum per unit mass increases. They get a spiral-like shape, moving out of their Schwarzschild or non-rotating GHSD black hole values and "looping in" towards some limiting frequency as the angular momentum per unit mass tends to its extremal value. For a given angular quantum number l, the number of spirals increases as the overtone number n increases. But for a given n, the increasing l has the effect of "unwinding" the spirals. It has been illustrated that both the real and imaginary parts of the frequencies are oscillatory functions of the angular momentum per unit mass a. The oscillation starts earlier and earlier as n grows for a fixed l, but it begins later and later as l increases for a fixed n.

We also study the dilaton-dependent relation to the quasinormal frequencies. It has been known that for the non-rotating GHSD black hole, the dilaton parameter D, which is related to the electric charge of this EMDA black hole, cannot make the frequencies spire in the complex ω plane, which is qualitatively different from the charge Q of the RN black hole. But for the rotating black hole, it is found that the frequencies generally move counterclockwise as the dilaton D decreases. They get a spiral-like shape, moving out of their rotating Kerr black hole values and "looping in" towards some limiting frequency as the dilaton tends to its extremal value. For a given angular quantum number l, we observe that the number of spirals increases as the overtone number n increases. But for a given overtone number n, the increasing l has the effect of "unwinding" the spirals. It is also illustrated that the real and imaginary parts of the quasinormal frequencies are the oscillatory functions of the dilaton D. The oscillation starts earlier and earlier as the angular momentum per unit mass a increases or the overtone number n grows for a fixed l, but it begins later and later as the angular quantum number l increases for a fixed n. It should be noted that the oscillatory functions of the angular momentum per unit mass a depend on the dilaton D, and the oscillation begins earlier and earlier as the dilaton D decreases. Thus, our study shows the qualitatively different properties between the dilaton spacetimes in string theory and those appearing in general relativity because of the appearance of dilaton.

JHEP01(2007)044

We give the so-call "Spiral-like Criterion" and point out that the frequencies won't spire in the complex ω plane if the heat capacity for the considered black hole is always negative and vice versa. However, the most interesting outcome of our investigation is that the critical point, at which the imaginary part of the wave function related to time-dependent part begins to oscillate obviously when the overtone number n grows to some value for a given quantum number l, is just the singular point of the heat capacity which is the second order phase transition point of Davies by comparing the singular point of the heat capacity with the critical point for this EMDA black hole. The fact seems to imply that there is some relation between the dynamical evolution and thermodynamic instabilities for the black hole which needs to be further investigated.

Acknowledgments

This work was supported by the National Natural Science Foundation of China under Grant No. 10473004; the FANEDD under Grant No. 200317; and the SRFDP under Grant No. 20040542003.

References

[1] K. Kokkotas and B. Schmidt, *Quasi-normal modes of stars and black hole*, *Living Reviews Relativ.* **2** (1999) 2 [gr-qc/9909058].

[2] V.P. Frolov and I.D. Novikov, *Black hole physics: basic concepts and new developments*, Dordrecht, Kluwer Academic, 1998.

[3] S. Hod, *Bohr's correspondence principle and the area spectrum of quantum black holes*, *Phys. Rev. Lett.* **81** (1998) 4293 [gr-qc/9812002].

[4] O. Dreyer, *Quasinormal modes, the area spectrum and black hole entropy*, *Phys. Rev. Lett.* **90** (2003) 081301 [gr-qc/0211076].

[5] J.M. Maldacena, *The large-N limit of superconformal field theories and supergravity*, *Adv. Theor. Math. Phys.* **2** (1998) 231 [*Int. J. Theor. Phys.* **38** (1999) 1113] [hep-th/9711200].

[6] E. Witten, *Anti-de Sitter space and holography*, *Adv. Theor. Math. Phys.* **2** (1998) 253 [hep-th/9802150].

[7] S. Kalyana Rama and B. Sathiapalan, *On the role of chaos in the AdS/CFT connection*, *Mod. Phys. Lett.* **A 14** (1999) 2635 [hep-th/9905219].

[8] T. Regge and J. Wheeler, *Stability of a Schwarzschild singularity*, *Phys. Rev.* **108** (1957) 1063.

[9] C.V. Vishveshwara, *Scattering of gravitational radiation by a Schwarzschild black-hole*, *Nature* **227** (1970) 936.

[10] W. Press, *Long wave trains of gravitational waves from a vibrating black hole*, *Astrophys. J.* **170** (1971) L105.

[11] S. Chandrasekhar and S. Detweller, *The quasi-normal modes of the Schwarzschild black hole*, *Proc. R. Soc. Lond. A* **344** (1975) 441.

[12] E.W. Leaver, *An analytic representation for the quasi-normal modes of Kerr black holes*, *Proc. R. Soc. Lond. A* **402** (1985) 285.

[13] H. Onozawa, T. Mishima, T. Okamura and H. Ishihara, *Quasinormal modes of maximally charged black holes*, *Phys. Rev.* **D 53** (1996) 7033 [gr-qc/9603021].

[14] E. Berti, V. Cardoso and S. Yoshida, *Highly damped quasinormal modes of Kerr black holes: a complete numerical investigation*, *Phys. Rev.* **D 69** (2004) 124018 [gr-qc/0401052].

[15] E. Berti and K.D. Kokkotas, *Quasinormal modes of Kerr-Newman black holes: coupling of electromagnetic and gravitational perturbations*, *Phys. Rev.* **D 71** (2005) 124008 [gr-qc/0502065].

[16] K.H.C. Castello-Branco, R.A. Konoplya and A. Zhidenko, *High overtones of Dirac perturbations of a Schwarzschild black hole*, *Phys. Rev.* **D 71** (2005) 047502 [hep-th/0411055].

[17] J.-L. Jing, *Dirac quasinormal modes of Schwarzschild black hole*, *Phys. Rev.* **D 71** (2005) 124006 [gr-qc/0502023].

[18] J.-L. Jing and Q.-Y. Pan, *Dirac quasinormal frequencies of the Kerr-Newman black hole*, *Nucl. Phys.* **B 728** (2005) 109 [gr-qc/0506098].

[19] J.-L. Jing, *Neutrino quasinormal modes of the Reissner-Nordström black hole*, *JHEP* **12** (2005) 005 [gr-qc/0512015].

[20] S. Chandrasekhar, *The mathematical theory of black holes*, Oxford University Press, 1983.

[21] R.A. Konoplya, *Quasinormal modes of the electrically charged dilaton black hole*, *Gen. Rel. Grav.* **34** (2002) 329 [gr-qc/0109096].

[22] R.A. Konoplya, *Decay of charged scalar field around a black hole: quasinormal modes of RN, RNAdS and dilaton black hole*, *Phys. Rev.* **D 66** (2002) 084007 [gr-qc/0207028].

[23] S.-B. Chen and J.-L. Jing, *Asymptotic quasinormal modes of a coupled scalar field in the Garfinkle-Horowitz-Strominger dilaton spacetime*, *Class. and Quant. Grav.* **22** (2005) 533 [gr-qc/0409013].

[24] S.-B. Chen and J.-L. Jing, *Dirac quasinormal modes of the Garfinkle-Horowitz-Strominger dilaton black-hole spacetime*, *Class. and Quant. Grav.* **22** (2005) 1129.

[25] S.-B. Chen and J.-L. Jing, *Asymptotic quasinormal modes of a coupled scalar field in the Gibbons-Maeda dilaton spacetime*, *Class. and Quant. Grav.* **22** (2005) 2159 [gr-qc/0511106].

[26] F.-W. Shu and Y.-G. Shen, *Quasinormal modes of charged black holes in string theory*, *Phys. Rev.* **D 70** (2004) 084046 [gr-qc/0410108].

[27] A. Garcia, D. Galtsov and O. Kechkin, *Class of stationary axisymmetric solutions of the Einstein-Maxwell dilaton - axion field equations*, *Phys. Rev. Lett.* **74** (1995) 1276.

[28] J.-L. Jing and S.-L. Wang, *Can Martinez's conjecture be extended to string theory?*, *Phys. Rev.* **D 65** (2002) 064001 [gr-qc/0110037].

[29] P.C.W. Davies, *The thermodynamic theory of black holes*, *Proc. Roy. Soc. Lond. A* **353** (1977) 499.

[30] P.C.W. Davies, *Thermodynamics of black holes*, *Rep. Prog. Phys.* **41** (1978) 1313.

JHEP01(2007)044

[31] P.C.W. Davies, *Thermodynamic phase transitions of Kerr-Newman black holes in de Sitter space*, *Class. and Quant. Grav.* **6** (1989) 1909.

[32] A. Ghosh and P. Mitra, *Entropy in dilatonic black hole background*, *Phys. Rev. Lett.* **73** (1994) 2521 [hep-th/9406210].

[33] W.H. Press, S.A. Teukolsky, B.P. Flannery and W.T. Vetterling, *Numerical recipes, the art of scientific computing*, New York, Cambridge University Press, 1986.

[34] J.-L. Jing, *Thermodynamics of stationary axisymmetric Einstein-Maxwell dilaton-axion black hole*, *Nucl. Phys.* **B 476** (1996) 548.

JHEP01(2007)044